# EFFECTS OF LATTICE DISTORTION, POLARON CONDUCTION AND DOUBLE-EXCHANGE INTERACTION ON THE PHYSICAL PROPERTIES OF MAGNETORESISTIVE MANGANITES AND COBALTITES

N.-C. YEH*, R. P. VASQUEZ**, J. Y. T. WEI*, C.-C. FU*, G. BEACH*, J. HUYNH*, A. V. SAMOILOV*, A. V. BORIS†, N. N. KOVALEVA†, and A. V. BAZHENOV†

*Department of Physics, California Institute of Technology, Pasadena, CA 91125

**Center for Space Microelectronics Technology, Jet Propulsion Laboratory, California Institute of Technology, Pasadena, CA 91109

† Institute of Solid State Physics, Russian Academy of Sciences, Chernogolovka, Moscow 142432, Russia

## ABSTRACT

The relevance of lattice distortion, polaron conduction, and double-exchange interaction to the occurrence of colossal magnetoresistance (CMR) is investigated by comparing the physical properties of magnetoresistive manganites and cobaltites. The samples studied in this work include epitaxial films and ceramics of manganites with both A- and B-site substitution, ($La_{0.7}Ca_{0.3}MnO_3$, $LaMn_{0.7}Ni_{0.3}O_3$, $LaMn_{0.5}Ni_{0.5}O_3$), as well as epitaxial films and ceramics of cobaltites ($La_{0.5}Ca_{0.5}CoO_3$). The structural, chemical, electrical transport, magnetic, optical properties and tunneling spectroscopy are studied. Based on our experimental results, we conclude that both double-exchange interaction and strong electron-phonon coupling due to the Jahn-Teller effect are essential to the occurrence of CMR.

## INTRODUCTION

Recent finding of colossal magnetoresistance (CMR) in the perovskite manganites $Ln_{1-x}A_xMnO_{3-\delta}$ (Ln: trivalent rare earth ions, A: divalent alkaline earth ions)[1-4] have led to renewed interest in the studies of these compounds which have been known for their rich magnetic properties. Various experimental investigations[1-6], particularly the giant oxygen isotope effect on the Curie temperature ($T_C$)[5] and the large reduction of magnetoresistance under a hydrostatic pressure[3], have lent supporting evidence for the important role of the strong electron-phonon coupling[7,8] in the magnetic and transport properties of these manganites.

To systematically investigate the effects of lattice distortion and Jahn-Teller coupling on the occurrence of CMR, we have recently studied $La_{0.7}Ca_{0.3}MnO_3$ (LCMO) and $La_{0.5}Ca_{0.5}CoO_3$ (LCCO) epitaxial films on different substrates of $LaAlO_3$ (LAO), $SrTiO_3$ (STO), and $YAlO_3$ (YAO)[9,10]. These substrates are chosen to provide a range of lattice constants which allows studies of the effects of tensile and compressive stress of the films. We find that there are two types of substrate-induced lattice distortion: One is the lattice strain ($\Delta a_0/a_0$) associated with the elastic deformation which influences the phonon modes and the magnetic exchange interaction; the other is the lattice relaxation ($\Delta a_s/a_s$) associated with the plastic deformation which induces extrinsic effects such as the formation of domain walls and dislocations, due to the lattice mismatch between the film and the substrate. Here the lattice strain is defined as the ratio of the difference between the film and bulk lattice constants relative to the bulk lattice constant ($a_0$), whereas



Mat. Res. Soc. Symp. Proc. Vol. 474 © 1997 Materials Research Society

the lattice relaxation is defined as the difference between the film and substrate lattice constants relative to the substrate lattice constant ($a_s$). Both the magnetoresistance and the zero-field resistivity of the manganites are strongly correlated with the substrate-induced lattice distortion[9,10], whereas similar lattice distortion in the cobaltites does not yield any significant effects on the magnetoresistance[9,10]. The correlation between the maximum magnetoresistance and the lattice distortion ($\Delta a_0/a_0$) and ($\Delta a_s/a_s$) in the LCMO epitaxial films is illustrated in Fig.1. Here the magnetoresistance is defined as $\Delta R_H \equiv [\rho(0) - \rho(H)]/\rho(H)$. The significantly different correlation with the lattice distortion between the magnetoresistance of LCMO and that of LCCO can be attributed to the Jahn-Teller effect and polaron conduction in the former.

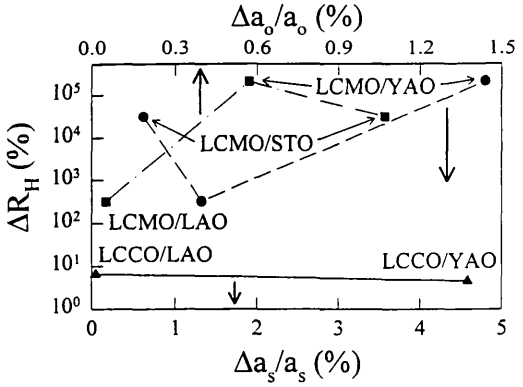


**Fig.1** Correlation of the magnetoresistance ($\Delta R_H$) and the substrate-induced lattice distortion in the manganites $La_{0.7}Ca_{0.3}MnO_3$ (LCMO). For comparison, the insignificant effect of lattice distortion on the magnetoresistance of the cobaltites $La_{0.5}Ca_{0.5}CoO_3$ (LCCO) is also illustrated.

In this work we present further experimental investigation of the physical properties of the LCMO and LCCO systems. We find that all measurements on the LCMO epitaxial films, including the electrical transport and optical reflectivity studies, are consistent with the presence of strong electron-phonon interaction in the manganites. Furthermore, the half-metallic electronic properties in the ferromagnetic state of LCMO also yield interesting spectroscopy associated with the spin-polarized tunneling. On the other hand, in spite of the small magnetoresistance, the multiple spin configurations of the Co-ions and the resulting "cluster glass"[11] in LCCO give rise to another interesting new phenomenon, the giant ferromagnetic Hall effect, with unprecedentedly large ferromagnetic Hall coefficient for a single-phase material[12]. To investigate the relevance of the double-exchange interaction to the occurrence of CMR, studies on the Ni-substituted manganites $LaMn_{0.7}Ni_{0.3}O_3$ and $LaMn_{0.5}Ni_{0.5}O_3$ (LMNO) are performed. These manganites with B-site doping are ferromagnets resulting from the superexchange interaction of the $Mn^{3+}$ and the low-spin $Ni^{III}$ Jahn-Teller ions[13-15]. Therefore by comparing the magnetoresistance of manganites with A- and B-site substitution, the role of double-exchange interaction in the CMR effect may be revealed.

## EXPERIMENTAL

The LCMO, LCCO and LMNO epitaxial films are grown by pulsed laser deposition using stoichiometric targets. For studying the substrate-induced lattice distortion, 200 nm thick films of LCMO and LCCO are grown on different (001) substrates at 700°C in 100 mTorr of oxygen, and subsequently annealed at 900°C of 1 atm oxygen for several hours. For comparing the relevance of the double-exchange interaction, the LMNO epitaxial films with 30% and 50% Ni-substitution are grown with similar conditions on the LAO substrates. The Curie temperature $T_C$ for LCMO is $260 \pm 10$ K, for LCCO $T_C = 180 \pm 5$ K, for LMNO with 50% Ni-substitution $T_C = 260 \pm 5$ K, and for LMNO with 30% Ni-substitution $T_C = 155 \pm 5$ K. The lattice constants $a$, $b$ and $c$ ($c \perp$ sample surface) as well as the epitaxy of the films are determined using high resolution x-ray diffraction (XRD) and x-ray rocking curves. The valence and core electronic states have been investigated with x-ray photoelectron spectroscopy (XPS). The electrical transport properties of these samples, including the zero-field resistivity, as well as the magnetoresistance and Hall effect, have been studied using conventional four-probe techniques with the van der Pauw correction[16]. Infrared reflectivity spectra of the LCMO epitaxial films have also been performed from 50 $cm^{-1}$ to 5000 $cm^{-1}$ by measuring both the optical reflectivity and transmittivity of the films on substrates and bare substrates[17]. The tunneling spectroscopy was performed with a low-temperature scanning-tunneling microscope (STM). These experimental results obtained from different measurements are given below.

## RESULTS

### Structural and Chemical Properties

The lattice constants and the corresponding lattice strain ($\Delta a_0/a_0$) and lattice relaxation ($\Delta a_s/a_s$) for the LCMO, LCCO and LMNO epitaxial films on various substrates are shown in Table I. All samples appear to be single-phase. The quality of epitaxy in the LCMO and LCCO films has been confirmed with x-ray rocking curves and has been demonstrated by the atomically smooth images of the surface topography and morphology

**Table I** The lattice constants, lattice relaxation and lattice strain determined from x-ray diffraction for $La_{0.7}Ca_{0.3}MnO_3$ (LCMO), $La_{0.5}Ca_{0.5}CoO_3$ (LCCO), $LaMn_{0.5}Ni_{0.5}O_3$ and $LaMn_{0.7}Ni_{0.3}O_3$ (LMNO) epitaxial films on substrates of $LaAlO_3$ (LAO), $YAlO_3$ (YAO), and $SrTiO_3$ (STO). For comparison, the room temperature lattice constants in Å for the bulk LCMO and LCCO are also tabulated, and the lattice constants for the substrates are: LAO [$a = b = c = 3.792$], STO [$a = b = c = 3.905$], and YAO [$(a/\sqrt{2}) = 3.662$, $(b/\sqrt{2}) = 3.768$, $(c/2) = 3.685$].

| Compound | Lattice | constant | (Å) | Lattice | Relaxation (%) | Lattice | Strain | (%) |
|---|---|---|---|---|---|---|---|---|
| | $(a/\sqrt{2})$ | $(b/\sqrt{2})$ | $(c/2)$ | $\Delta a_s/a_s$ | $\Delta b_s/b_s$ | $\Delta a_0/a_0$ | $\Delta b_0/b_0$ | $\Delta c_0/c_0$ |
| LCMO | 3.840 | 3.890 | 3.860 | — | — | — | — | — |
| LCMO/LAO | 3.842 | 3.854 | 3.921 | 1.32 | 1.64 | 0.05 | −0.93 | 1.58 |
| LCMO/STO | 3.881 | 3.927 | 3.845 | 0.62 | 0.56 | 1.07 | 0.95 | −0.39 |
| LCMO/YAO | 3.862 | 3.886 | 3.899 | 4.80 | 3.08 | 0.57 | −0.10 | 1.01 |
| LCCO | 3.797 | 3.797 | 3.797 | — | — | — | — | — |
| LCCO/LAO | 3.790 | 3.790 | 3.793 | −0.05 | −0.05 | −0.18 | −0.18 | −0.11 |
| LCCO/YAO | 3.828 | 3.823 | 3.777 | 4.59 | 1.41 | 0.82 | 0.68 | −0.53 |
| LMNO/LAO (x=0.3) | — | — | 3.884 | — | — | — | — | — |
| LMNO/LAO (x=0.5) | — | — | 3.881 | — | — | — | — | — |

taken with our STM, as reported in Ref.[10].

Among both the LCMO and LCCO films of the same thickness, we find the largest lattice distortion in LCMO/YAO and LCCO/YAO from the x-ray data[9]. The chemical properties of these samples are further characterized with x-ray photoelectron spectroscopy (XPS)[18]. The room-temperature valence band spectra show no density of states at the Fermi level for the LCMO and LMNO, and a high density of states at the Fermi level for the LCCO, as illustrated in Fig.2(a), consistent with the semiconducting and insulating nature of the LCMO and LMNO, respectively, and the metallic nature of LCCO. More details of the XPS data taken on the LCCO films have been given elsewhere[18]. Here we provide new results on the LMNO films in Fig.2(b) which compare the La 3d and Ni 2p signals of $LaMn_{1-x}Ni_xO_3$ ($x$ = 0, 0.3, 0.5). The structure in each spin-orbit split component of the La 3d signal reflects strong mixing of final states with $\underline{3d^9}4f^0\underline{L}$ and $\underline{3d^9}4f^1\underline{L}$ character, where underscoring denotes a hole and L denotes the oxygen ligand. The increased intensity of the high binding energy component of the La $3d_{3/2}$ signal with increase Ni substitution results from overlap with the Ni $2p_{3/2}$ signal. The Ni $2p_{1/2}$ signal occurs at a binding energy of 872.2 eV, which is consistent with $Ni^{3+}$ as measured in $LaNiO_3$[19]. The Ni $2p_{1/2}$ signal of $Ni^{2+}$ in NiO occurs at a lower binding energy of 871.3 eV and exhibits a prominent satellite peak at higher binding energy[20] which is not apparent in the spectra in Fig.2(b). We can therefore conclude that the substitutional Ni is into the +3 oxidation state and does not dope carriers in the manganites, consistent with the observed high resistivity. Further support for this finding is shown in the valence band spectra in Fig.2(a), in which the increase in Ni 3d states near 2 eV with increased Ni substitution is apparent, but does not result in a clear Fermi edge cutoff which would be expected with metallic conductivity.

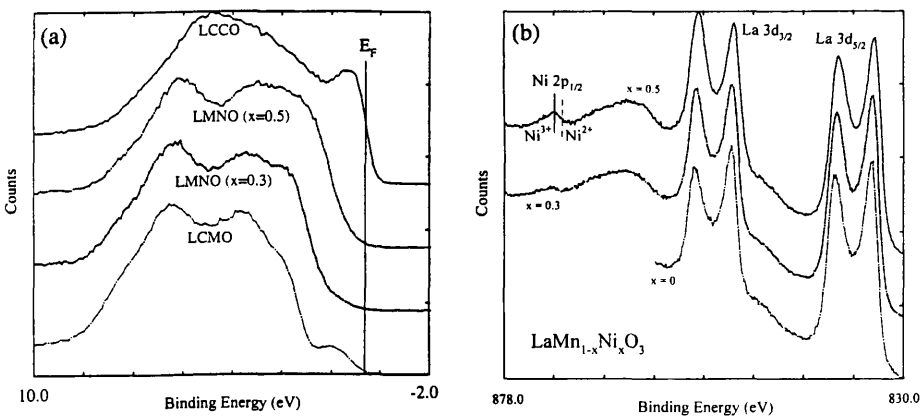


**Fig.2** **(a)** The room-temperature valence band spectra of the LCMO, LCCO and LMNO films on LAO substrates. We note the absence of any density of states at the Fermi level for the LCMO and LMNO, and a high density of states at the Fermi level for the LCCO. **(b)** The La 3d and Ni 2p signals of the $LaMn_{1-x}Ni_xO_3$ ($x$ = 0, 0.3, 0.5) films. We note that the La 3d signal reflects strong mixing of final states with $\underline{3d^9}4f^0\underline{L}$ and $\underline{3d^9}4f^1\underline{L}$ character, and that the Ni $2p_{1/2}$ signal occurs at a binding energy of 872.2 eV, consistent with $Ni^{3+}$ as measured in $LaNiO_3$[19].

## Electrical Transport Properties

The effects of lattice distortion on the electrical transport properties of LCMO films on substrates of LAO, STO and YAO have been published elsewhere[9,10], and the correlation of the maximum magnetoresistance $\Delta R_H$ with the lattice distortion $\langle \Delta a/a \rangle$ has been summarized in Fig.1. Here we compare the effects of Jahn-Teller coupling and double-exchange interaction on the occurrence of CMR by comparing the zero-field and finite-field (6 Tesla) resistivity ($\rho$) vs. temperature ($T$) data of the films of LCMO, LCCO and LMNO films on LAO substrates, as illustrated in Fig.3. We note that in Fig.3(a) the LCMO system exhibits a resistive peak at $T_p$ where $T_p < T_C$, and the corresponding magnetoresistance $\Delta R_H$ given in the inset is the largest among all films on the LAO substrate. We also note that the high-temperature resistivity can be described in terms of the small polaron model, with a polaron binding energy $E_b \approx 0.35$ eV[9], comparable to the Jahn-Teller coupling energy[7].

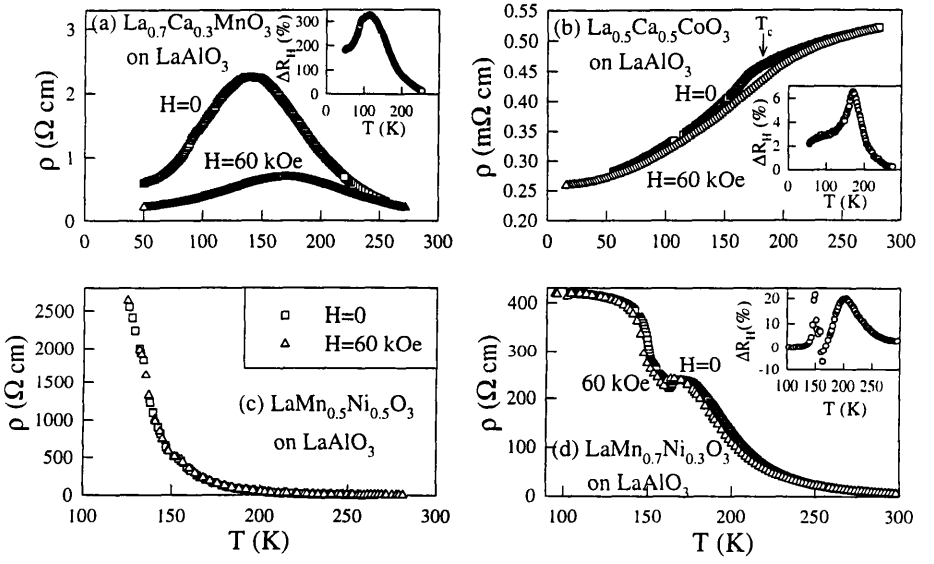


**Fig.3** Comparison of the resistivity $\rho$ at $H = 0$ and $H = 6$ Tesla as a function of the temperature ($T$) for **(a)** $La_{0.7}Ca_{0.3}MnO_3$, **(b)** $La_{0.5}Ca_{0.5}CoO_3$, **(c)** $LaMn_{0.5}Ni_{0.5}O_3$, and **(d)** $LaMn_{0.7}Ni_{0.3}O_3$ epitaxial films on $LaAlO_3$ substrates. The insets illustrate the magnetoresistance $\Delta R_H$-vs.$T$ data for all four samples.

More specifically, we find that the resistivity data for all LCMO films can be described according to the expression:

$$\rho(T) \approx \alpha T \exp\left[\frac{E_b}{k_B T}\right], \tag{1}$$

where $E_b \approx 0.35$ eV[9]. This energy compares favorably to the Jahn-Teller coupling en-

ergy[6], suggesting that the high-temperature conduction mechanism is dominated by the lattice polaron conduction. On the other hand, the low temperature transport properties appear to be strongly correlated with the degree of lattice distortion. That is, samples of larger lattice distortion exhibit larger resistivity and magnetoresistance, as illustrated in Fig.1, suggesting increasing scattering of carriers due to a larger number of magnetic domains and grain boundaries induced by larger lattice distortion.

In contrast to the peak feature in the $\rho$-vs.-$T$ data of the LCMO system, the LCCO sample reveal monotonic temperature dependence in the resistivity, as illustrated in Fig.3(b), with orders of magnitude better electrical conduction. The zero-field resistivity has a anomalous change of slope at $T_C$, and the magnetoresistance peak occurs at approximately the same temperature, suggesting that the suppression of the spin-disorder scattering in the magnetically ordered state due to either high fields or low temperatures is the origin of magnetoresistance in LCCO.

The LMNO samples both appear to be insulating, (Fig.3(c) and Fig.3(d)), and the sample with 30% Ni-substitution is less resistive than that with 50% Ni-substitution, showing an anomalous drop in resistivity near $T_C$ before increasing again with further decrease in temperature, as shown in Fig.3(d). This small reduction in resistivity at $T \sim 150$ K $\ll T_C \approx 240$ K may be related to the presence of a small percentage of $Mn^{4+}$ and $Ni^{2+}$ ions[15] which contribute excess carriers, so that the conductivity is enhanced as the disorder-spin scattering is suppressed at $T \ll T_C$. This conjecture is also consistent with the finite magnetoresistance in the $LaMn_{0.7}Ni_{0.3}O_3$ epitaxial film where the presence of a small percentage of $Mn^{4+}$ and $Ni^{2+}$ ions[15] results in incomplete ferromagnetic ordering[13,14], so that the resistivity may be reduced by the application of an external magnetic field which suppresses the spin disorder and enhances the carrier

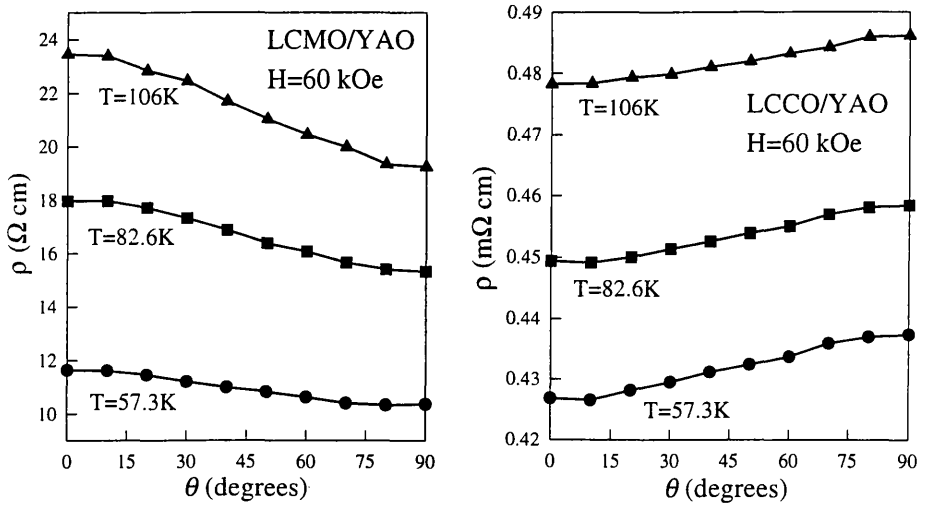


**Fig.4** The anisotropic resistivity of LCMO/YAO and LCCO/YAO films at various temperatures below $T_C$ and for $H = 6$ Tesla.

hopping conduction. We note that the Ni-ions are believed to be in the low-spin state with the electronic configuration of $t_{2g}^6 e_g^1$[13,14], so that both the $Mn^{3+}$ and $Ni^{III}$ ions are Jahn-Teller ions. The superexchange interaction between the $Mn^{3+}$ and $Ni^{III}$ ions[14,15] gives rise to a moderate ferromagnetic exchange interaction[13].

In Fig.4 we show the anisotropic magnetoresistance at $T < T_C$ in LCMO/YAO and LCCO/YAO samples as a function of the angle $\theta$ between the applied magnetic field and the thin film surface. It is interesting to note the opposite angular dependence in these two samples, despite the fact that both samples have comparable lattice distortion, as shown in Table I. A possible explanation for the significant anisotropic resistivity (up to 25%) of the LCMO/YAO sample may be related to the polaron conduction. That is, for $\vec{H}$ parallel to the substrate ($\theta = 90°$), spins become much better aligned below $T_C$ and therefore the larger magnetization reduces the polaron unbinding energy, giving rise to better conductivity. On the other hand, for the LCCO/YAO film, the small increase of resistivity (up to 2%) as $\vec{H}$ is rotated from the c-axis to the ab-plane may be explained by the significant substrate-induced reduction of the c-axis lattice constant and the increase of the a and b-axis lattice constants (see Table I). The lattice distortion thus induced might favor stronger double-exchange interaction for fields aligned along c-axis ($\theta = 0$) than for fields parallel to the ab-plane ($\theta = 90°$), hence the smaller resistivity for $\vec{H} \parallel \hat{c}$.

## Magnetic Properties

The spontaneous magnetization ($M_s$) vs. temperature ($T$) data for the bulk LCMO and LCCO samples are shown in Fig.5(a). To examine the temperature dependence of $M_s$ near $T_C$, we find that

$$M_s(T \to T_C) = M_{s0}(1 - T/T_C)^{\beta}, \tag{2}$$

where the critical exponent $\beta = 0.50 \pm 0.01$ is consistent with the mean-field theory for ferromagnets[21]. In addition, the first harmonic of the longitudinal magnetic susceptibility

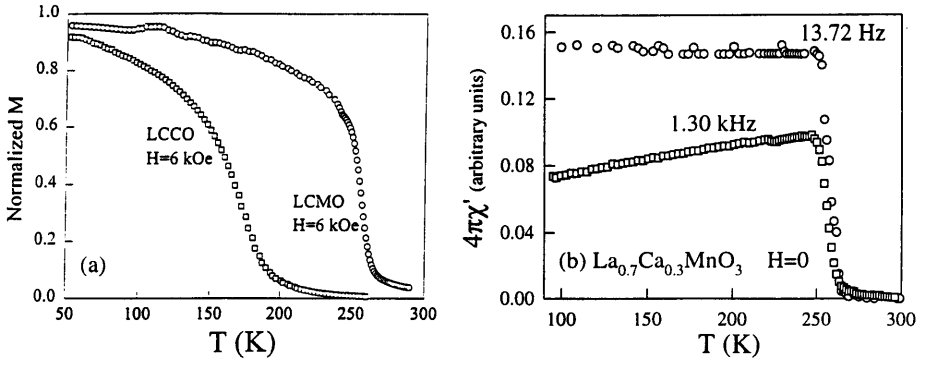


**Fig.5** **(a)** The magnetization ($M$) vs. temperature ($T$) data for bulk LCMO and LCCO samples. **(b)** The real part of the ac magnetic susceptibility ($4\pi\chi'$) vs. temperature ($T$) data taken at frequencies $f = 13.72$ Hz and $f = 1.30$ kHz and for $H = 0$.

($\chi$) at two frequencies $f$ = 13.72 Hz and $f$ = 1.30 kHz is shown in Fig.5(b). It is interesting to note that the real part of the high-frequency ac magnetic susceptibility ($\chi'$) of LCMO is slightly reduced relative to that of the low-frequency susceptibility, and the low-temperature high-frequency $\chi'$ increases slightly until near $T_C^-$, and then drops rapidly at $T_C$. The frequency dependence of $\chi'$ in the ferromagnetic state may be understood in terms of spin relaxation induced by a longitudinal ac excitation[22].

## Optical Properties

The effects of substrate-induced lattice strain on the optical phonon modes have been revealed by our recent infrared reflectivity studies[17], and the frequency shifts of the phonon modes are consistent with the XRD results[9,10]. As reported in Ref.[17], we find that the substrate-induced lattice strain has strong influence on the Mn-O stretching and Mn-O-Mn bending phonon modes, and has practically no effect on the La (Ca) vibrational mode. Furthermore, the frequency of the Mn-O stretching mode and that of the Mn-O-Mn bending mode show much stronger power-law dependence on the lattice constants ($\omega \propto a^{-8}$ for the stretching mode and $\omega \propto a^{-5}$ for the bending mode) than that of the conventional dependence ($\omega \propto a^{-3/2}$)[23]. In Fig.6, the ratio of the frequency shift ($-\Delta\omega/\omega$) relative to the lattice strain ($\Delta a/a$) for the stretching and the bending modes are illustrated. These large optical frequency shifts in the Mn-O phonon modes due to the substrate-induced lattice strain are suggestive of strong electron-phonon coupling in the LCMO system.

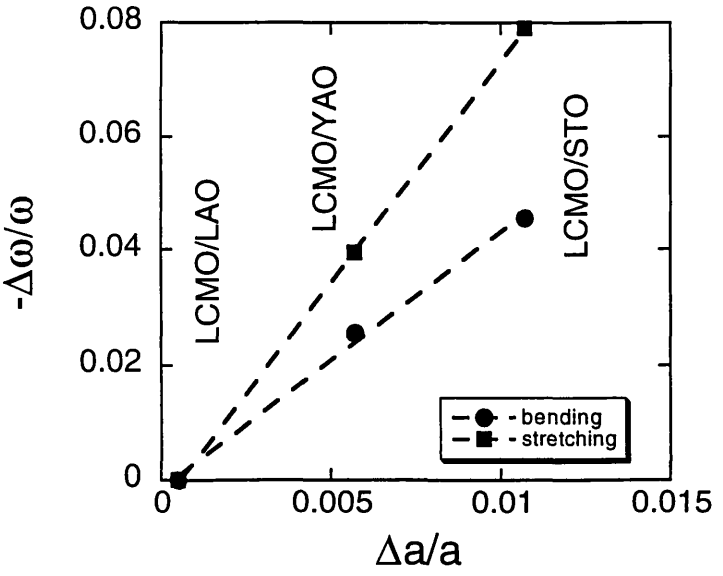


**Fig.6** Correlation of the ratio of the phonon frequency shift ($-\Delta\omega/\omega$) and the substrate-induced lattice strain ($\Delta a/a$) for the Mn-O stretching and Mn-O-Mn bending modes in LCMO epitaxial films[17].

## Tunneling Spectroscopy

Tunneling spectroscopy was performed on $La_{0.7}Ca_{0.3}MnO_3$ (LCMO) and $LaMnO_3$ (LMO) films with a variable-temperature scanning tunneling microscope (STM), using a platinum tip as counter-electrode. Typical junction impedance was $\sim$ 10MΩ, with the bias voltage applied to the sample. The current vs. voltage $I$-$V$ data was converted into the normalized tunneling conductance $[(dI/dV)(I/V)^{-1} - 1]$ according to the procedure developed by Feenstra et al.[24]. Figure 7 shows the conductance spectra for LCMO at 77 K, well below the Curie temperature ($T_c \approx$ 260 K). Pronounced peaks are present at $\sim \pm 1.75$ V, bearing notable resemblance to the spin-split density-of-states spectrum (shown in inset) calculated for the itinerant Mn $3d$ and O $2p$ bands in the ferromagnetic state[25]. The peaks are absent at room temperature for LCMO in the paramagnetic state[26], as well as for the undoped LMO[26] which shows no CMR behavior. This overall consistency offers strong evidence of a half-metallic band structure for LCMO in the ferromagnetic state, and implicates spin-splitting of the itinerant electrons as playing a key role in CMR[25,26].

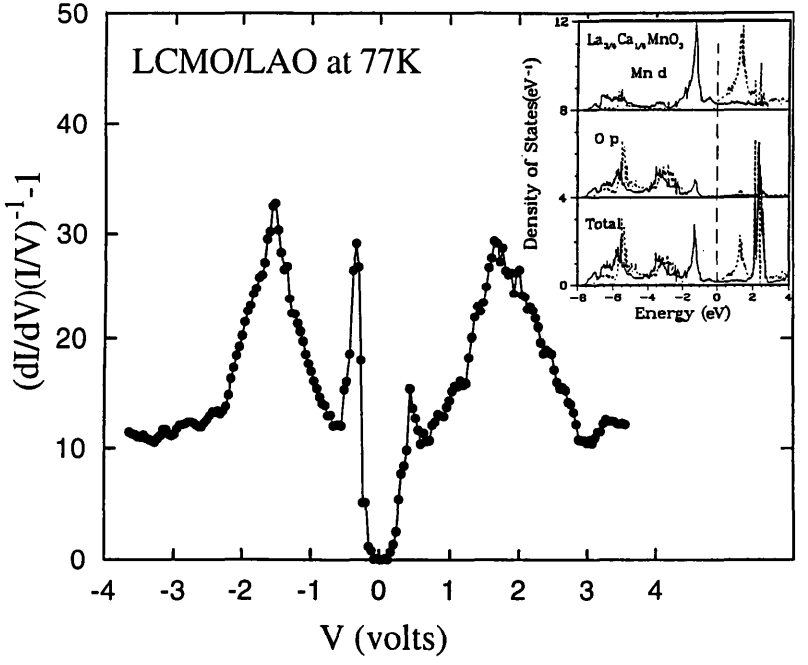


**Fig.7** The normalized tunneling conductance $[(dI/dV)(I/V)^{-1} - 1]$ vs. the bias voltage ($V$) of an LCMO/LAO film taken at $T$ = 77 K using a low-temperture STM, well below the Curie temperature ($T_C$ = 260 K). The pronounced peaks at $\sim \pm 1.75$ V are consistent with the spin-split density-of-states spectrum given in Ref.[25] for LCMO in the ferromagnetic state, and the gap-like structure with sharp peaks at $\sim$ 0.35 eV may be associated with the Jahn-Teller splitting[9,26].

Also noticeable in the conductance spectrum for LCMO at 77 K is a gap-like structure, with sharp peaks at $\sim \pm 0.35$ eV. This gap feature is absent for LCMO at room temperature, but also present in the data for LMO[26]. It seems plausible to attribute this gap feature to evidence for Jahn-Teller splitting which, according to the band structure calculations, should exist in LCMO at low temperatures as well as in the undoped LMO[26]. Such evidence would be consistent with the models for CMR involving polaron conduction[7], and is also in excellent agreement with the polaron unbinding energy derived from our electrical transport data[9].

## DISCUSSION

Our experimental results which compare LCMO, LCCO and LMNO systems are suggestive of the importance of both double-exchange interaction and Jahn-Teller coupling to the occurrence of CMR. As summarized in Table II, different combinations of the double-exchange interaction, Jahn-Teller coupling, and superexchange interaction in these three families of ferromagnetic perovskites yield various interesting and distinct physical properties for each system. For instance, the large effects of substrate-induced lattice distortion on the magnetoresistance[9,10], optical conductivity and phonon frequencies[17] in LCMO can be attributed to the strong electron-phonon coupling associated with the Jahn-Teller effect and the presence of the double-exchange interaction in LCMO[7]. The multiple spin configurations and the double-exchange interaction of the Co ions in LCCO are known to yield the "cluster-glass" like behavior[27] with enhanced spin fluctuations, which may be responsible for the giant ferromagnetic Hall effect observed in LCCO[12]. On the other hand, the small magnetoresistance in LCCO suggests that spin fluctuations in a system with highly mobile conducting carriers do not result in CMR[9]. The insulating behavior and the small magnetoresistance of the LMNO system may be attributed to the superex-

**Table II** Comparison of the physical properties of $La_{0.7}Ca_{0.3}MnO_3$, $La_{0.5}Ca_{0.5}CoO_3$, and $LaMn_{1-x}Ni_xO_3$ ($x = 0.3, 0.5$) epitaxial films on $LaAlO_3$ substrates.

| Perovskite | Physical effects | Phenomena |
|---|---|---|
| $La_{0.7}Ca_{0.3}MnO_3$ on $LaAlO_3$ | - Jahn-Teller effect<br>- double exchange interaction<br>- half-metallic bands below $T_C$ | - significant CMR (larger CMR from larger lattice distortion)<br>- strong optical phonon frequency shift with large lattice strain (Boris et al.) |
| $La_{0.5}Ca_{0.5}CoO_3$ on $LaAlO_3$ | - absence of Jahn-Teller effect<br>- double exchange interaction | - small $\Delta R_H$<br>- giant ferromagnetic Hall effect (due to multi-spin states) (Samoilov et al.) |
| $LaMn_{1-x}Ni_xO_3$ on $LaAlO_3$ | - Jahn-Teller effect<br>- superexchange interaction | - high resistivity insulator<br>- small $\Delta R_H$ |

change interaction, and the small enhancement of the conductivity at low temperatures in the LMNO system with 30% Ni-substitution may be related to the existence of a small percentage of the $Mn^{4+}$ and $Ni^{2+}$ ions, in addition to the predominant $Mn^{3+}$ and $Ni^{III}$ ions. These mixed valences resemble the multiple spin configurations in LCCO, the latter being responsible for the giant ferromagnetic Hall effect without significant enhancement to the magnetoresistance.

Finally, we comment on the important physics implications of our direct evidence for the half-metallic band structures below $T_C$ in LCMO, from the tunneling spectroscopy. The significant exchange energy splitting ($\sim$ 3.5 eV) between the majority and minority bands[25] with bandwidths ($\sim$ 1.0 eV) narrower than this energy splitting implies that the electrical conduction is only associated with the majority band and the carrier spins are completely polarized[25,26,28]. The half-metallic behavior in the ferromagnetic state has an important consequence on the low-temperature zero-field resistivity and the finite-field magnetoresistance. That is, in the presence of magnetic domains, either due to chemical effects such as inhomogeneous cation distributions or lattice distortion effects such as grain boundaries and dislocations, the electrical conduction from one domain to another may be severely impeded if the spins are not aligned. The application of an external magnetic field can align the spins in different magnetic domains, thereby substantially lowering the energy barrier for the conduction carriers between domains and significantly reducing the resistivity. This phenomenon is in contrast to most ferromagnetic metals in which the degree of spin polarization is small (*e.g.*, 10% in Ni) and the misalignment of spins among different domains does not result in an energy barrier for the electrical conduction[25,28].

## CONCLUSION

The effects of lattice distortion, Jahn-Teller coupling, and double-exchange interaction on the occurrence of colossal magnetoresistance (CMR) are investigated by comparing the physical properties of $La_{0.7}Ca_{0.3}MnO_3$ (LCMO), $La_{0.5}Ca_{0.5}CoO_3$ (LCCO), $La(Mn_{0.7}Ni_{0.3})O_3$, and $La(Mn_{0.5}Ni_{0.5})O_3$ (LMNO) epitaxial films on various substrates. Our studies reveal that both the double exchange and Jahn-Teller effects are important to the occurrence of CMR. In addition, our tunneling spectroscopy of LCMO at $T \ll T_C$ is consistent with the half-metallic band structure calculations, suggesting the spin-splitting of the itinerant electrons may play a key role in CMR.

## ACKNOWLEDGEMENT

The research at Caltech is supported by the Packard Foundation and the National Aeronautics and Space Administration, Office of Space Science (NASA/OSS), and the Caltech President's Fund. Part of the research was performed by the Center for Space Microelectronics Technology, Jet Propulsion Laboratory, Caltech, and was sponsored by NASA/OSS. We thank Nikko Hitech International Inc. for supplying the $YAlO_3$ substrates used in this work.

## REFERENCES

1. R. von Hemlolt, J. Wecker, B. Holzapfel, L. Schultz, and K. Samwer, Phys. Rev. Lett. **71**, 2331 (1993).
2. S. Jin et al., Science **264**, 413 (1994); Appl. Phys. Lett. **66**, 382 (1995); Appl. Phys. Lett. **67**, 557 (1995).

3. H. Y. Hwang et al., Phys. Rev. Lett. **75**, 914 (1995).
4. Y. Moritomo et al., Phys. Rev. **B51**, 16491 (1995); K. Khazeni et al., Phys. Rev. Lett. **76**, 295 (1996).
5. M. R. Ibarra et al., P. A. Algarabel, C. Marquina, J. Blasco, and J. Garcia, Phys. Rev. Lett. **75**, 3541 (1995).
6. G.-M. Zhao, K. Conder, H. Keller, and K. A. Müller, Nature **381**, 676 (1996).
7. A. J. Millis, P. B. Littlewood, and B. I. Shraiman, Phys. Rev. Lett. **74**, 5144 (1995); A. J. Millis, B. I. Shraiman, and R. Mueller, Phys. Rev. Lett. **77**, 175 (1996).
8. P. Dai, J. D. Zhang, H. A. Mook, S. H. Liou, P. A. Dowben et al., Phys. Rev. **B54**, 3694 (1996); M. Jaime, M. B. Salamon, K. Pettit, M. Rubinstein, R. E. Treece et al., Appl. Phys. Lett. (1996).
9. N.-C. Yeh, R. P. Vasquez, D. A. Beam, C.-C. Fu, J. Huynh, and G. Beach, J. Phys.: Condens. Matter, (1997). (in press).
10. N.-C. Yeh, C. C. Fu, J. Y. T. Wei, R. P. Vasquez, J. Huynh, S. M. Maurer, and G, Beach, J. Appl. Phys. **81**, (1997).
11. J. B. Goodenough, A. Wold, R. J. Arnott, and N. Menyuk, Phys. Rev. **124**, 373 (1961); J. B. Goodenough, in "*Progress in Solid State Chemistry*", Vol. 5, Pergamon Press (1971), ed. by H. Reiss.
12. A. V. Samoilov, N.-C. Yeh, and R. P. Vasquez, preprint (1997); "*Epitaxial Oxide Thin Films III*", Mater. Res. Soc. Proc., San Francisco, (1997).
13. J. B. Goodenough, A. Wold, R. J. Arnott, N. Menyuk, Phys. Rev. **124**, 373 (1961).
14. N. Y. Vasanthacharya, P. Ganguly, J. B. Goodenough, and C. N. R. Rao, J. Phys. C: Solid State Phys. **17**, 2745 (1984).
15. A. Wold, R. J. Arnott, and J. B. Goodenough, Phys. Rev. **29**, 387 (1958).
16. L. J. van der Pauw, Phillips Res. Reports **13**, 1 (1958).
17. A. V. Boris, N. N. Kovaleva, A. V. Bazhenov, A. V. Samoilov, N.-C. Yeh and R. P. Vasquez, J. Appl. Phys. **81**, (1997).
18. R. P. Vasquez, Phys. Rev. **B54**, 14938 (1996).
19. S. R. Barman, A. Chainani, D. D. Sarma, Phys. Rev. **B49**, 8475 (1994).
20. J. F. Moulder, W. F. Stickle, P. E. Sobol, and K. D. Bomben., "*Handbook of X-ray Photoelectron Spectroscopy*", Perkin-Elmer corp., Eden Prairie, MN (1992).
21. See, for example, S. K. Ma, "*Modern Theory of Critical Phenomena*", Addison-Wesley, (1976).
22. R. M. White, "*Quantum Theory of Magnetism*", Springer-Verlag, Berlin Heidelberg, (1983).
23. See, for example, C. Kittel, "*Introduction to Solid State Physics*", 6th edition.
24. R. M. Feenstra, J. A. Stroscio, A. P. Fein, Surf. Sci. **181**, 295 (1987).
25. W. E. Pickett and D. J. Singh, Phys. Rev. **B53**, 1146 (1996).
26. J. Y. T. Wei, N.-C. Yeh, and R. P. Vasquez, to be published.
27. M. A. Senaris-Rodriguez, J. B. Goodenough, J. Solid State Chem. **118**, 323 (1995).
28. H.Y. Hwang, S.-W. Cheong, N.P. Ong, B. Batlogg, Phys.Rev.Lett. **77**, 2041 (1996).